Strong Mechanical Squeezing in a quadratically coupled Optomechanical MIM System

PH 518: Project Report - II

A project report submitted in partial fulfillment
of the requirements for the degree of
Master of Science in Physics
by

Priyankar Banerjee
(202121032)
Supervised by
Prof. Amarendra Kumar Sarma

Department of Physics
Indian Institute of Technology, Guwahati

DECLARATION

I hereby declare that the work presented in this report titled **Strong Mechanical Squeezing in a quadratically coupled cavity Optomechanical MIM System** submitted by me for the evaluation of PH518 coursework in Semester IV in the Master of Science, Physics program at IIT Guwahati, is an authentic record of the work carried out under the guidance of **Prof. Amarendra Kumar Sarma**. Due references and acknowledgments have been given in the report to all the materials used.

Priyankar Banerjee
Department of Physics
Indian Institute of Technology, Guwahati Date: 25.04.22

CERTIFICATE

This is to certify that the above information given by the candidate is correct to the best of my knowledge.

Prof. Amarendra Kumar Sarma Date: 25.04.22

Acknowledgements

This work would not have been possible without the great support of many people. First and foremost, I would like to express my gratitude to Prof. Amarendra Kumar Sarma, for providing me an opportunity to work under him for the M.Sc. Project and for suggesting this interesting open problem to work on. I would really like to thank him for his optimism during the course for my work and for giving me enough freedom at every point in the journey. This helped me learn how to independently solve problems.

Secondly, I would like to thank Mr. Sampreet Kalita, PhD student at the Department of Physics, IIT Guwahati for his constant support. He has been an ever-supportive senior who helped me in various ways during my research. Our multiple conversations revolved around a wide range of topics, not just stipulated to research and they were really insightful.

I am grateful to a bunch of really supportive friends at IIT Guwahati, who made this M.Sc. journey a memorable one.

Finally and most importantly, I would like to thank my Mother for her unconditional support and sacrifices for me. She is the one who keeps motivating me no matter how hard the times become.

April, 2022 Priyankar Banerjee

Contents

List of Figures **5**

1 Introduction **7**

2 Theory **10**
2.1 Quantization of the EM field 10
2.1.1 Canonically conjugate pair for an EM field 10
2.1.2 Correspondence with the quantum version 12
2.2 Concept of Quadratures 12
2.3 Quadrature squeezing 13

3 Optomechanical MIM System **14**
3.1 Setting up the system 14
3.1.1 Rotating Frame 15
3.2 Equations of motion 16
3.2.1 Classical solution of the equation of motion 16

4 Generation of Mechanical Squeezing **18**
4.1 Rotating wave approximation 18
4.2 Without Rotating Wave Approximation 20
4.3 Covariance Matrix 20
4.4 Routh-Hurwitz Criterion 20
4.5 Squeezing as a result of competing effect of two parameters 22
4.6 Optimal side-band ratio 25

5 Analytical and Numerical Solutions **26**
5.1 Analytical Solution (under Adiabatic Approximation) 26
5.2 Numerical Solution 27

6 Discussion **31**

Appendices **32**

A Table of variable definitions **33**

B Steady state fluctuation of the mechanical mode **34**

C Position fluctuation spectra of the mechanical mode **36**

7 Bibliography **38**

List of Figures

3.1 Schematic diagram representing the membrane-in-middle optomechanical system 14

4.1 The variance in fluctuations of position and momentum quadratures with time 22
4.2 (a) Variance in Position Quadrature $\langle \delta \hat{\tilde{X}}_b^2 \rangle$ and (b) the number of atoms in the Bogoliubov Modes $\hat{\beta}$ plotted with respect to the ratio of the coupling strengths of the side-bands 24
4.3 (a) Maximized Variance in Position Quadrature $\langle \delta \hat{\tilde{X}}_b^2 \rangle$ and (b) Optimal side-band ratio $\frac{G_1}{G_0}$ plotted with respect to the coupling strength of the side-band 25

5.1 Variance in Position Quadrature $\langle \delta \hat{\tilde{X}}_b^2 \rangle$ obtained from the approximate solution 27
5.2 Variance in Position Quadrature $\langle \delta \hat{\tilde{X}}_b^2 \rangle$ obtained from numerical solution 28
5.3 Optimal ratio of the side-band strength plotted with respect to the side-band 29
5.4 Steady state variance in position quadrature $\langle \hat{\tilde{X}}_b^2 \rangle_s$ is plotted with varying occupancy of the mechanical mode 29

Abstract

The minimum energy of a quantum harmonic oscillator is constrained by the ever-present "zero-point" fluctuations of the quantum ground state. However, squeezing lets us exploit Heisenberg's uncertainty principle to reduce the noise of a single quadrature below this threshold at the cost of increased fluctuations in the other.
This report explores a scheme to generate strong mechanical squeezing in a laser-driven membrane-in-the-middle cavity by introducing a periodic modulation in the driving amplitude. The motivation for this work comes from a work by Kronwald et al. [1], where they propose a method for dissipative generation of bosonic squeezing. The squeezing achieved is much more robust in the optomechanical MIM system considered in this report compared to previous works [2].
The periodic modulation of the driving field amplitude causes the optomechanical coupling parameter to take a specific form. We show that an optimal choice of the ratio of side-bands of this coupling parameter exists, which gives rise to an enhanced squeezing. We also show that the Bogoliubov modes of the mechanical oscillator cool down to its ground state, resulting in an effective squeezing well beyond the 3-dB standard quantum limit (SQL). We then verify these results analytically (under the adiabatic approximation) and numerically. Finally, we explore the robustness of the degree of squeezing obtained and show that it is below the SQL up to a thermal occupancy of 10^4 phonons.

Chapter 1

Introduction

Cavity quantum optomechanics is the study of a mechanical system's interaction with electromagnetic radiation via the radiation pressure force. Many experiments in this domain are aimed at preparing and controlling a mechanical element to enter a quantum state of motion. This allows us to test quantum mechanics' fundamental hypotheses at a mesoscopic level. By making these quantum objects larger and larger, we can subsequently study quantum effects of fundamental forces at a macroscopic level. Apart from that, a cavity optomechanical system's mechanical oscillator is particularly sensitive to minor displacements caused by very small forces. This makes such systems a potential candidate to be used in making quantum-enhanced sensors in future that would help us in making ultra-small measurements.
The Heisenberg's uncertainty principle sets a limit to how precise a measurement can be. This is one of the fundamental principles of quantum physics. For position $\hat{x}$ and momentum $\hat{p}$ of an object or a particle,

$$\Delta\hat{x}^2\Delta\hat{p}^2 \geq \frac{|\langle[\hat{x},\hat{p}]\rangle|^2}{4} = \frac{\hbar^2}{4} \tag{1.1}$$

The uncertainty principle also leads to the non-zero ground state energy of quantum harmonic oscillator. The Hamiltonian is given as,

$$\hat{H} = \frac{\hat{p}^2}{2m} + \frac{1}{2}m\omega_m^2\hat{x}^2 \tag{1.2}$$

Since, $\hat{x}^2 \geq \Delta\hat{x}^2$ and $\hat{p}^2 \geq \Delta\hat{p}^2$, the energy of the oscillator is,

$$\begin{aligned}\langle\hat{H}\rangle = E &\geq \frac{\Delta\hat{p}^2}{2m} + \frac{1}{2}m\omega_m^2\Delta\hat{x}^2 \\ &\geq \frac{\hbar^2}{8m\Delta\hat{x}^2} + \frac{1}{2}m\omega_m^2\Delta\hat{x}^2\end{aligned} \tag{1.3}$$

The zero-point energy occurs when $\Delta\hat{x} = \sqrt{\frac{\hbar}{2m\omega_m}}$, which becomes $E = \frac{1}{2}\hbar\omega_m$. This $\Delta\hat{x}$ is the called zero-point position fluctuation, which means that even in the ground

state the position will always have fluctuations with variance $\Delta\hat{x}^2_{zpf} = \frac{\hbar}{2m\omega_m}$.
The precision of position measurements of a mechanical oscillator is limited by this zero point fluctuation. Many interferometric detectors, including the LIGO [3], and VIRGO [4], employ mechanical resonators as part of their setup. For these, zero-point fluctuations set a lower limit on the mechanical elements' lowest detectable displacement. To add on that, measuring such small displacements may itself add noise to the system. The minimum amount of noise while measuring position is quantified by the standard quantum limit.
Most position measuring systems, in fact, have noise contributions that exceed this limit. This position operator $\hat{x}$ may be divided into two non-commuting quadrature operators with the same uncertainty relation as Eq. (1.1). By squeezing the motion of the mechanical oscillator, it should be feasible to measure beyond the "standard quantum limit" while avoiding zero-point fluctuations in a single quadrature at the expense of an increased noise in the other. In both the optical and mechanical modes of the cavity optomechanical system squeezed states can be created and leading to such non-commuting observable pairs getting squeezed.
The thermal occupancy and accompanying position fluctuations of the mechanical mode are substantially higher than the quantum zero-point fluctuations, which is a serious problem for quantum squeezing, even at a relatively low temperature. There are many theoretical schemes that have been proposed to produce squeezing below the 3 dB level. However, squeezing below the zero-point fluctuation is yet to be experimentally achieved.
In this dissertation, we implement a mechanical squeezing scheme for the dissipative generation of a squeezed quantum state in a quadratically coupled optomechanical system by periodically modulating the driving amplitude. This method closely relates to the approach of Bai et. al. [2] that was recently used to produce strong mechanical squeezing in a standard optomechanical system consisting of an optical cavity coupled to a movable mirror driven by an external field. Squeezing via specific kind of pump modulation has advantages over other methods, as it causes the optomechanical coupling to take a specific form which causes the bogoliubov mode to cool down via dissipative interaction with the cavity mode.
The report is laid out as follows: In Chapter 2, I breifly introduce the concept the concept of EM field quantization and explain in brief what is meant by quadratures, both of optical as well as the mechanical mode of the system. In Chapter 3, I develop the theory of the membrane-in-middle cavity optomechanical (MIM) system and then look at the dynamic behaviour of the system by deriving the equation of motions. Then in Chapter 4, I look at the squeezing in the position quadrature of the mechanical mode and explain the squeezing effect as a competing effect between two opposite behaviours. Then I go on to optimize the ratio of the side-bands in the coupling which produces maximum squeezing. Next, in Chapter 5 I analyze the system approximately as well as find the exact solution numerically to study squeezing of the position quadrature, and then go on the study the robustness of the squeezing achieved. Lastly, Appendix A includes definitions of variables used throughout the report. Appendix B contains the

calculation for the steady state fluctuation of the mechanical mode calculated using the adiabatic approximation and Appendix C contains the derivation for the expression of position fluctuation spectrum of the mechanical mode.

Chapter 2

Theory

We will begin by briefly introducing the concept of quantization of the electromagnetic field which is central to many phenomena occurring at a quantum scale as vacuum fluctuations and squeezing of the optical mode in a cavity-optomechanical system. Then, we go on to discuss the concept of quadratures pertaining to both optical field as well as an mechanical oscillator. Though, our aim is to study quadrature squeezing of the mechanical mode, we will start by introducing these concepts in context of the optical mode before moving on the mechanical mode.

2.1 Quantization of the EM field

The semi-classical approach to the physics of electromagnetic field interacting with matter is not quite efficient in explaining the quantum phenomena underlined above. The EM field needs to be quantized for these concepts to be meaningful. Here we introduce the concept of canonical quantization of an electromagnetic field using which we can write the field as a combination of two canonically conjugate variables.

2.1.1 Canonically conjugate pair for an EM field

In free space, the Maxwell's equations are given as:

$$\begin{aligned} \vec{\nabla} \cdot \vec{E}(\vec{r}, t) &= 0 \\ \vec{\nabla} \cdot \vec{B}(\vec{r}, t) &= 0 \\ \vec{\nabla} \times \vec{E}(\vec{r}, t) &= -\frac{\partial}{\partial t} \vec{B}(\vec{r}, t) \\ \vec{\nabla} \times \vec{B}(\vec{r}, t) &= \frac{1}{c^2} \frac{\partial}{\partial t} \vec{E}(\vec{r}, t) \end{aligned} \tag{2.1}$$

Here, $\vec{E}$ and $\vec{B}$ form a set of coupled variables, which are continuous in nature. Now, to canonically quantize the EM field, we need a set of conjugate variable pairs which are decoupled and discrete in nature.

We can rewrite Maxwell's equations in terms of the potentials, the scalar potential ϕ and the vector potential $\vec{A}$. But if we choose a special gauge for these kind of potentials, the so-called Coulomb gauge, then we can describe the E-field and B-field in this situation purely through a vector potential. So we introduce the vector potential $\vec{A}(\vec{r},t)$ and from this vector potential we can derive all the electric and magnetic fields in the system in the situation we are discussing here. In this so-called Coulomb gauge, where $\vec{\nabla}\cdot\vec{A}=0$,

$$\begin{aligned}\vec{B}(\vec{r},t) &= \vec{\nabla}\times\vec{A}(\vec{r},t)\\ \vec{E}(\vec{r},t) &= -\frac{\partial\vec{A}}{\partial t}\end{aligned} \tag{2.2}$$

So. $\vec{A}$ contains all the information about the B- and E-fields in our system. So, now the question we can ask is what kind of dynamical equations govern the evolution of this vector potential field, $\vec{A}(\vec{r},t)$. Calculating, the curl of $\vec{B}$ from Eq. (2.2) and putting in Eq. (2.1)(d),

$$\begin{aligned}\vec{\nabla}\times(\vec{\nabla}\times\vec{A}) &= -\frac{1}{c^2}\frac{\partial^2}{\partial t^2}\vec{A}\\ \vec{\nabla}^2\vec{A}-\frac{1}{c^2}\frac{\partial^2}{\partial t^2}\vec{A} &= 0\end{aligned} \tag{2.3}$$

So, this represents the wave equation with wave velocity being the speed of light. The general plane wave solution can be simply written as,

$$\vec{A}_{\vec{k},\alpha}(\vec{r},t) = \vec{\epsilon}_{\vec{k},\alpha}A_{\vec{k},\alpha}e^{i(\vec{k}\cdot\vec{r}-\omega_k t)} \tag{2.4}$$

Here, $\vec{\epsilon}_{\vec{k},\alpha}$ is the polarization vector (with polarization component α and wave vector $\vec{k}$), $A_{\vec{k},\alpha}$ is the complex amplitude of the field and the rest is the phase component (with ω_k as the frequency of the radiation field). If we would have an infinite space, then the $\vec{k}$ vectors would be continuous. However, we want to discuss is the situation where we confine the radiation field to a box (i.e. we introduce periodic boundary conditions), requiring that the allowed field solutions are same in every direction. This requires that the phase factors of this vector potential also follow the same. So. the allowed modes of the field are

$$k_x = \frac{2\pi}{L}n_x,\; k_y = \frac{2\pi}{L}n_y,\; k_z = \frac{2\pi}{L}n_y \tag{2.5}$$

Now we can write a general solution of the vector potential, $\vec{A}(\vec{r},t)$ simply as a Fourier decomposition of all of those modes.

$$\vec{A}(\vec{r},t) = \sum_{\vec{k},\alpha}\epsilon_{\vec{k},\alpha}(A_{\vec{k},\alpha}e^{i(\vec{k}\cdot\vec{r}-\omega_k t)} + A^*_{\vec{k},\alpha}e^{-i(\vec{k}\cdot\vec{r}-\omega_k t)}) \tag{2.6}$$

From here, the we can also calculate the electric and the magnetic field using Eq. (2.2),

$$\begin{aligned}\vec{E}(\vec{r},t) &= -\frac{\partial\vec{A}}{\partial t} = \sum_{\vec{k},\alpha}\epsilon_{\vec{k},\alpha}i\omega_k(A_{\vec{k},\alpha}e^{i(\vec{k}\cdot\vec{r}-\omega_k t)} - A^*_{\vec{k},\alpha}e^{-i(\vec{k}\cdot\vec{r}-\omega_k t)})\\ \vec{B}(\vec{r},t) &= \vec{\nabla}\times\vec{A}(\vec{r},t) = \sum_{\vec{k},\alpha}i(\vec{k}\times\epsilon_{\vec{k},\alpha})(A_{\vec{k},\alpha}e^{i(\vec{k}\cdot\vec{r}-\omega_k t)} - A^*_{\vec{k},\alpha}e^{-i(\vec{k}\cdot\vec{r}-\omega_k t)})\end{aligned} \tag{2.7}$$

Energy of this radiation field is given by,

$$H_R = \frac{\epsilon_0}{2}\int_V d^3r[\vec{E}^2(\vec{r},t) + c^2\vec{B}^2(\vec{r},t)] = \sum_{\vec{k},\alpha}\epsilon_0 V\omega_k^2[A_{\vec{k},\alpha}A^*_{\vec{k},\alpha} + A^*_{\vec{k},\alpha}A_{\vec{k},\alpha}] \tag{2.8}$$

2.1.2 Correspondence with the quantum version

We know that each radiation field mode has attached to it a quantum harmonic oscillator. So we just have to sum over all those quantum harmonic oscillators to get the total radiation field Hamiltonian $\hat{H}_R = \sum_k \hat{H}_k$, where

$$\hat{H}_k = \frac{1}{2}\hbar\omega_k(\hat{a}_k\hat{a}_k^\dagger + \hat{a}_k^\dagger\hat{a}_k) \tag{2.9}$$

Here, $\hat{a}_k^\dagger$ and $\hat{a}_k$ are the creation and annihilation operators of the k^{th} mode. If we compare the energy stored in the kth mode of the quantum harmonic oscillator Eq. (2.9), with the classical expression Eq. (2.8), we can make a simple correspondence between the quantum and the classical versions

$$\begin{aligned} A_k &\to \sqrt{\frac{\hbar}{2\epsilon_0 V\omega_k}}\hat{a}_k \\ A_k^* &\to \sqrt{\frac{\hbar}{2\epsilon_0 V\omega_k}}\hat{a}_k^\dagger \end{aligned} \tag{2.10}$$

Now, that we have established a formal correspondence between the quantum and the classical picture, we can identify the classical canonically conjugate variables, where

$$\begin{aligned} \vec{E}(\vec{r},t) &= \sum_k i\vec{\epsilon}_k\sqrt{\frac{\hbar\omega_k}{2\epsilon_0 V}}(\hat{a}_k e^{i(\vec{k}\cdot\vec{r}-\omega_k t)} - \hat{a}_k^\dagger e^{-i(\vec{k}\cdot\vec{r}-\omega_k t)}) \\ \vec{B}(\vec{r},t) &= \sum_k i\sqrt{\frac{\hbar}{2\epsilon_0 V\omega_k}}(\vec{k}\times\vec{\epsilon}_k)(\hat{a}_k e^{i(\vec{k}\cdot\vec{r}-\omega_k t)} - \hat{a}_k^\dagger e^{-i(\vec{k}\cdot\vec{r}-\omega_k t)}) \end{aligned} \tag{2.11}$$

2.2 Concept of Quadratures

We now introduce the concept of quadratures, using which we can write the electric field amplitude for a single mode k from Eq. (2.7) as,

$$\begin{aligned} E_k(\vec{r},t) &= i\sqrt{\frac{\hbar\omega_k}{2\epsilon_0 V}}(A_k e^{i(\vec{k}\cdot\vec{r}-\omega_k t)} - A_k^* e^{-i(\vec{k}\cdot\vec{r}-\omega_k t)}) \\ \Rightarrow E_k(\vec{r},t) &= -\sqrt{\frac{\hbar\omega_k}{\epsilon_0 V}}(X_k\sin\Big(\vec{k}\cdot\vec{r}-\omega_k t\Big) + Y_k\cos\Big(\vec{k}\cdot\vec{r}-\omega_k t\Big)) \end{aligned} \tag{2.12}$$

Here, we have introduced the quadrature components as $X_k = \frac{A_k + A_k^*}{\sqrt{2}}$ and $Y_k = \frac{i[A_k^* - A_k]}{\sqrt{2}}$. Thus, we can represent the field on a complex plane, using these coordinates X_k and Y_k. This

vector (X_k, Y_k) rotates with an angular frequency ω_k.
Analogously, we can similarly define quadratures in the quantum mechanical picture. For a single mode k, electric field is

$$\hat{E}_k = i\epsilon_k \sqrt{\frac{\hbar\omega_k}{2\epsilon_0 V}}(\hat{a}e^{i(\vec{k}\cdot\vec{r}-\omega_k t)} - \hat{a}_k^\dagger e^{-i(\vec{k}\cdot\vec{r}-\omega_k t)}) \tag{2.13}$$

Now, here the quadratures are defined as the position quadrature $\hat{X}_k = \frac{\hat{a}_k+\hat{a}_k^\dagger}{\sqrt{2}}$ and the momentum quadrature $\hat{Y}_k = \frac{i[\hat{a}_k^\dagger-\hat{a}_k]}{\sqrt{2}}$, so that the field can be re-written as,

$$\hat{E}_k(\vec{r},t) = -\sqrt{\frac{\hbar\omega_k}{\epsilon_0 V}}(\hat{X}_k \sin\Big(\vec{k}\cdot\vec{r}-\omega_k t\Big) + \hat{Y}_k \cos\Big(\vec{k}\cdot\vec{r}-\omega_k t\Big)) \tag{2.14}$$

The quadratures represent quantum mechanical observables and are hermitian operators. Since, these operators do not commute ($[\hat{X}_k, \hat{Y}_k] = i$), we cannot precisely obtain both the observables at the same time. The uncertainties in measuring the quadrature operators in some arbitrary state ψ follows,($(\Delta\hat{\mathcal{O}})^2 = \langle\psi|\hat{\mathcal{O}}^2|\psi\rangle - \langle\psi|\hat{\mathcal{O}}|\psi\rangle^2$) ,

$$\Delta\hat{X}_k \cdot \Delta\hat{Y}_k \geq \frac{1}{2}|\langle\psi|[\hat{X}_k, \hat{Y}_k]|\psi\rangle| = \frac{1}{2} \tag{2.15}$$

Now, the position or momentum of the mechanical resonator of an optomechanical system can be decomposed into two orthogonal motional quadratures (say, $\hat{X}$ and $\hat{Y}$). The position operator can be written in terms of these quadratures as $\hat{x} = x_{zpf}(\hat{X}\cos\omega_m t + \hat{Y}\sin\omega_m t)$, where ω_m is the motional frequency of the mechanical element of the optomechanical system. These quadratures also satisfy a similar inequality as seen in Eq. (2.15). These non-commuting quadratures define a set of axes rotating through the position-momentum space at a frequency ω_m.

2.3 Quadrature squeezing

The laser field and the mechanical oscillator in an optomechanical system interact non-linearly. If this non-linear coupling is strong enough, it leads to the generation of non-gaussian states. An important non-classical effect that is shown in such optomechanical systems in squeezing of the optical or the mechanical modes.
As opposed to optical modes, which are in ground state even at room temperature, the thermal occupancy of the mechanical mode is much higher even at very low temperature. Hence, quantum squeezing can be achieved only when we can overcome this large thermal contribution [5].
Throughout this dissertation, we will explore a way to reduce the fluctuations in position quadrature of the mechanical oscillator in a cavity-optomechanical system.

Chapter 3

Optomechanical MIM System

First, we'll develop the theory of the membrane-in-middle cavity optomechanical system by considering a setup consisting of one fabry-perot cavity with two fixed mirrors on either side which is detuned by the motion of a thin membrane oscillating in between them. Then, we will look at the dynamic behaviour of the system by deriving the equations of motion which govern its time evolution.

3.1 Setting up the system

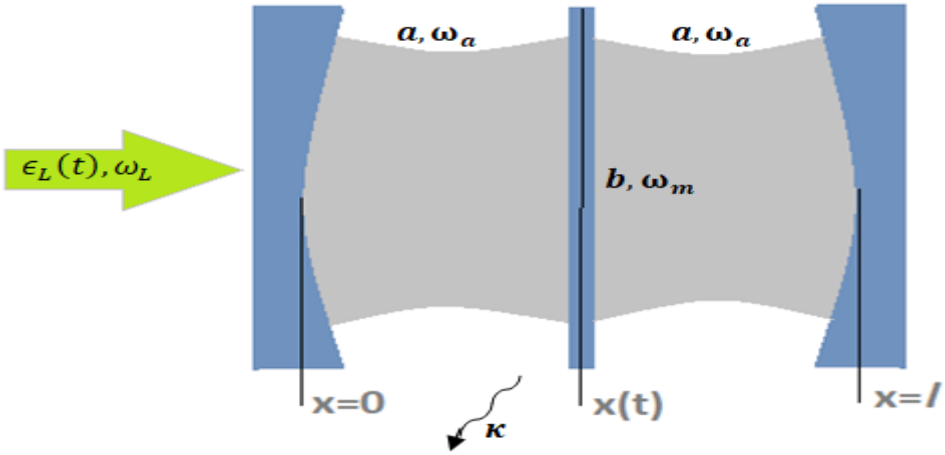

Figure 3.1: Schematic diagram representing the membrane-in-middle optomechanical system, where the cavity field is periodically driven by a periodically amplitude-modulated external laser field which couples to the membrane via the controllable radiation-pressure interaction.

Upon driving the system by a laser field, a pressure is exerted by the photons on the movable membrane inside the cavity, thus changing the cavity length on either side of it. This in turn modulates the resonant frequency of the cavity ω_a. If we consider the length of the cavity to be l, the membrane is displaced by a distance x and c is the speed of light, then the new ω_a

becomes $\frac{N\pi c}{l+x}$. Using Taylor expansion, for $x \ll l$,

$$\omega_a(x) \approx \omega_{a0}(1 - \frac{x}{l}) \tag{3.1}$$

Here, $\omega_{a0} = \frac{N\pi c}{l}$ is the initial resonant frequency of the cavity mode in the absence of a drive. Now, let's construct the Hamiltonian of this system. Considering the cavity and the mechanical mode as quantum harmonic oscillators, oscillating with a frequency ω_a and ω_m respectively, in the absence of any driving, we can write

$$\hat{H}_{OM} = \omega_a(x)\hat{a}^\dagger\hat{a} + \omega_m\hat{b}^\dagger\hat{b} \tag{3.2}$$

where $\hat{a}$ is the annihilation operator of the cavity photons, and $\hat{b}$ is the annihilation operator of the oscillating membrane. Substituting Eq. (3.1) in Eq. (3.2),

$$H_{OM} = \omega_a\hat{a}^\dagger\hat{a} + \omega_m\hat{b}^\dagger\hat{b} - g\hat{a}^\dagger\hat{a}(\hat{b}^\dagger + \hat{b})^2 \tag{3.3}$$

where $g = \frac{\omega_a}{l}x_{zpf}$ is the optomechanical coupling strength. We have Taylor expanded $\omega_a(x)$ around an extremum (as $x = 0$) such that $\omega_a(x)|_{x=0} = \omega_a(0) + \frac{1}{2}\omega_a''(0)x^2$, where the position quadrature of the mechanical mode $x = x_{zpf}(\hat{b} + \hat{b}^\dagger)$, where $x_{zpf} = \sqrt{\frac{\hbar}{2m\omega_m}}$ is the zero-point fluctuation of the membrane. The first order term $\omega_a'(0)$ in the Taylor expansion of $\omega_a(x)$ is zero, because of the symmetric contribution of the laser field on both sides of the membrane. If the membrane is displaced $+x$ amount on one side, the cavity length on either side of it will either increase or decrease by a magnitude x, which causes the linear term to vanish.
The coupling strength is negligible when compared to the frequency of the mechanical mode, which makes it hard to show the desired quantum effects. Hence, we drive the system using a laser, in order to get a strong optomechanical coupling. Now, the optomechanical Hamiltonian is of form:

$$\hat{H} = \omega_a\hat{a}^\dagger\hat{a} + \omega_m\hat{b}^\dagger\hat{b} - g\hat{a}^\dagger\hat{a}(\hat{b}^\dagger + \hat{b})^2 + i\epsilon_L(t)(\hat{a}^\dagger e^{-i\omega_L t} - \hat{a}e^{i\omega_L t}) \tag{3.4}$$

where $\epsilon_L(t) = \sum_{-\infty}^{\infty}\epsilon_n e^{-in\Omega t}$ is the periodically modulated amplitude of the external driving field with a modulation frequency Ω and ω_L is the frequency of the external driving field.

To make sure the classical mean value fluctuation of the mechanical mode is non-zero, we add a constant force of aplitude $\eta\ \omega_m$ to the membrane. This requires an additional term $\eta\omega_m(\hat{b}^\dagger + \hat{b})$ in the Hamiltonian. Finally, the optomechanical Hamiltonian for the MIM system driven by a periodically laser field with the membrane initially displaced is given as,

$$\hat{H} = \omega_a\hat{a}^\dagger\hat{a} + \omega_m\hat{b}^\dagger\hat{b} - g\hat{a}^\dagger\hat{a}(\hat{b}^\dagger + \hat{b})^2 + i\epsilon_L(t)(\hat{a}^\dagger e^{-i\omega_L t} - \hat{a}e^{i\omega_L t}) + \eta\omega_m(\hat{b}^\dagger + \hat{b}) \tag{3.5}$$

3.1.1 Rotating Frame

Now to simplify our calculations, we can switch to a reference frame rotating at a frequency ω_L. For this we apply the rotation transformation of form $\hat{U} = e^{-i\omega_L\hat{a}^\dagger\hat{a}}$ and calculate $\hat{U}^\dagger\hat{H}\hat{U} - \hbar\omega_L\hat{a}^\dagger\hat{a}$ to rewrite Eq. (3.5) as

$$\hat{H} = \delta_a\hat{a}^\dagger\hat{a} + \omega_m\hat{b}^\dagger\hat{b} - g\hat{a}^\dagger\hat{a}(\hat{b}^\dagger + \hat{b})^2 + i\epsilon_L(t)(\hat{a}^\dagger - \hat{a}) + \eta\omega_m(\hat{b}^\dagger + \hat{b}) \tag{3.6}$$

Here, $\delta_a = \omega_a - \omega_L$ corresponds to the frequency detuning of the cavity.

3.2 Equations of motion

In order to study the system dynamics, we will now look at the time evolution of the system operators using Heisenberg equations of motion. We have to take into account the dissipation of the cavity mode and the decay of the mechanical resonator. We also take into account the thermal noise, which is present in the system due to the mechanical resonator coupled to the thermal bath.

$$\begin{aligned}\dot{\hat{a}} &= \frac{1}{i\hbar}[\hat{a}, \hat{H}] - [\hat{a}, \hat{a}^\dagger](\frac{\kappa}{2}\hat{a} - \sqrt{\kappa}\hat{a}_{in}(t)) \\ \dot{\hat{b}} &= \frac{1}{i\hbar}[\hat{b}, \hat{H}] - [\hat{b}, \hat{b}^\dagger](\frac{\gamma_m}{2}\hat{b} - \sqrt{\gamma_m}\hat{b}_{in}(t))\end{aligned} \tag{3.7}$$

In the R.H.S, the first term represents the time evolution of the field operators, the second term represents the decay of the bosonic mode and the last term represents the noise entering the system owing to the coupling of the system with the thermal bath. κ is the cavity dissipation rate and γ_m is the dissipation rate of the mechanical mode. $\hat{a}_{in}(t)$ and $\hat{b}_{in}(t)$ are respectively the noise operators associated with the cavity and mechanical dissipation.
For our quadratically coupled optomechanical set-up, the quantum langevin equations are of form,

$$\begin{aligned}\dot{\hat{a}} &= -i\delta_a\hat{a} + ig_a\hat{a}(\hat{b}^\dagger + \hat{b})^2 + \epsilon_L(t) - \frac{\kappa}{2}\hat{a} + \sqrt{\kappa_a}\hat{a}_{in}(t) \\ \dot{\hat{b}} &= -i\omega_m\hat{b} + 2ig_a\hat{a}^\dagger\hat{a}(\hat{b}^\dagger + \hat{b}) - i\eta\omega_m - \frac{\gamma_m}{2}\hat{b} + \sqrt{\gamma_m}\hat{b}_{in}(t)\end{aligned} \tag{3.8}$$

The correlation functions for these noise operators which are assumed to have a gaussian nature are given as $\langle\hat{\mathcal{O}}^\dagger_{in}(t)\hat{\mathcal{O}}_{in}(t')\rangle = \int d\omega\langle\hat{\mathcal{O}}^\dagger_{in}\hat{\mathcal{O}}_{in}\rangle e^{i\omega(t-t')}$ [6]. We get,

$$\begin{aligned}\langle\hat{a}^\dagger_{in}(t)\hat{a}_{in}(t')\rangle &= \int d\omega\langle\hat{a}^\dagger_{in}\hat{a}_{in}\rangle e^{i\omega(t-t')} = n_a\delta(t-t') \\ \langle\hat{a}_{in}(t)\hat{a}^\dagger_{in}(t')\rangle &= (n_a+1)\delta(t-t') \\ \langle\hat{b}^\dagger_{in}(t)\hat{b}_{in}(t')\rangle &= n_m\delta(t-t') \\ \langle\hat{b}_{in}(t)\hat{b}^\dagger_{in}(t')\rangle &= (n_m+1)\delta(t-t')\end{aligned} \tag{3.9}$$

Where, n_m and n_a are the number of atoms in the mechanical and cavity mode respectively.

3.2.1 Classical solution of the equation of motion

The QLEs obtained in Eq. (3.8) can be linearized by assuming the operators representing the cavity and mechanical mode ($\hat{a}$ and $\hat{b}$) are equal to the sum of its classical expectation value and the fluctuation, $\mathcal{O} = \langle\mathcal{O}\rangle + \delta\mathcal{O}$. Then, writing down the equation of the expectation values $\langle\hat{a}(t)\rangle$ and $\langle\hat{b}(t)\rangle$:

$$\begin{aligned}\frac{d\langle\hat{a}(t)\rangle}{dt} &= -i\delta_a\langle\hat{a}(t)\rangle + ig_0\langle\hat{a}(t)\rangle(\langle\hat{b}(t)\rangle + \langle\hat{b}(t)\rangle^*)^2 + \epsilon_L(t) - \frac{\kappa}{2}\langle\hat{a}(t)\rangle \\ \frac{d\langle\hat{b}(t)\rangle}{dt} &= -i\omega_m\langle\hat{b}(t)\rangle + 2ig_0|\langle\hat{a}(t)\rangle|^2(\langle\hat{b}(t)\rangle + \langle\hat{b}(t)\rangle^*) - i\eta\omega_m - \frac{\gamma_m}{2}\langle\hat{b}(t)\rangle\end{aligned} \tag{3.10}$$

Now, we can extract the linearized equations of the quantum fluctuations from Eq. (3.8) by removing the classical mean values of the system operators:

$$\dot{\hat{a}} \simeq -i\Delta_a\hat{a} + 2ig_o\langle\hat{a}\rangle(\langle\hat{b}(t)\rangle + \langle\hat{b}(t)\rangle^*)(\hat{b} + \hat{b}^\dagger) - \frac{\kappa}{2}\hat{a} + \sqrt{\kappa}\hat{a}_{in}(t) \tag{3.11}$$

$$\dot{\hat{b}} \simeq -i\omega_m\hat{b} + 2ig_o(\langle\hat{a}\rangle^*\hat{a} + \langle\hat{a}\rangle\hat{a}^\dagger)(\langle\hat{b}(t)\rangle + \langle\hat{b}(t)\rangle^*) + 2ig_0|\langle\hat{a}(t)\rangle|^2(\hat{b} + \hat{b}^\dagger) - \frac{\gamma_m}{2}\hat{b} + \sqrt{\gamma_m}\hat{b}_{in}(t) \tag{3.12}$$

Here, the detuning parameter Δ_a is equal to $\delta_a - g_0(\langle\hat{b}(t)\rangle + \langle\hat{b}(t)\rangle^*)^2$.

Chapter 4

Generation of Mechanical Squeezing

According to the Floquet theorem, due to the periodically modulated amplitude of the external driving $\epsilon_L(t)$ [7], the amplitude of the cavity and mechanical mode ($\langle\hat{a}(t)\rangle$ and $\langle\hat{b}(t)\rangle$) in the long time limit achieve the same oscillation frequency.
To produce the desired dynamics, only three side-band terms in $\epsilon_L(t) = \sum_{-\infty}^{\infty} \epsilon_n e^{-in\Omega t}$ are considered (i.e. $\epsilon_{-1}e^{i\Omega t}+\epsilon_0+\epsilon_1 e^{-i\Omega t}$). In the limit $t \to \infty$ the cavity mode and the mechanical mode amplitude would show the same behaviour as the modulated external field. Hence, we define the expectation values of the annihilation operator of the cavity and mechanical mode as:

$$\begin{aligned} \langle\hat{a}(t)\rangle &= \alpha = a_{-1}e^{i\Omega_1 t} + a_0 + a_1 e^{-i\Omega_1 t} \\ \langle\hat{b}(t)\rangle &= \beta = b_{-1}e^{i\Omega_2 t} + b_0 + b_1 e^{-i\Omega_2 t} \end{aligned} \tag{4.1}$$

4.1 Rotating wave approximation

Now, we indicate the fluctuation operators as

$$\begin{aligned} \hat{a} &= \hat{\tilde{a}}e^{-i\Delta_a t} \quad \text{and} \quad \hat{a}_{in} = \hat{\tilde{a}}_{in}e^{-i\Delta_a t} \\ \hat{b} &= \hat{\tilde{b}}e^{-i\omega_m t} \quad \text{and} \quad \hat{b}_{in} = \hat{\tilde{b}}_{in}e^{-i\omega_m t} \end{aligned} \tag{4.2}$$

Here, effective cavity detuning Δ_a and external driving frequency $\Omega_{1(2)}$ are set to be ω_m and $2\omega_m$ respectively.
Substituting Eq. (4.2) and Eq. (4.1) in the QLEs, we see that few terms are highly oscillatory whereas others are stationary with respect to the rotating frame. Considering a weak optomechanical coupling between the sidebands, we can set the non-stationary terms to zero. This is called the rotating wave approximation (RWA). Under RWA Eq. (3.11) and Eq. (3.12) can rewritten as,

$$\begin{aligned} \dot{\hat{\tilde{a}}} &\simeq 2ig_0[((a_{-1}+a_1)(b_{-1}+b_1)+2a_0b_0)\hat{\tilde{b}} + (a_0(b_{-1}+b_1)+2a_1b_0)\hat{\tilde{b}}^\dagger] - \frac{\kappa}{2}\hat{\tilde{a}} + \sqrt{\kappa}\hat{\tilde{a}}_{in} \\ \dot{\hat{\tilde{b}}} &\simeq 2ig_0[((a_{-1}+a_1)(b_{-1}+b_1)+2a_0b_0)\hat{\tilde{a}} + (a_0(b_{-1}+b_1)+2a_1b_0)\hat{\tilde{a}}^\dagger] \\ &\quad + 2ig_0[(a_{-1}^2+a_0^2+a_1^2)\hat{\tilde{b}} + (a_0a_1+a_0a_{-1})\hat{\tilde{b}}^\dagger] - \frac{\gamma_m}{2}\hat{\tilde{b}} + \sqrt{\gamma_m}\hat{\tilde{b}}_{in} \end{aligned} \tag{4.3}$$

We simplify things and write Eq. (4.3) as,

$$\begin{aligned}\dot{\hat{\tilde{a}}} &= iG_0\hat{\tilde{b}} + iG_1\hat{\tilde{b}}^\dagger - \frac{\kappa}{2}\hat{\tilde{a}} + \sqrt{\kappa}\hat{\tilde{a}}_{in} \\ \dot{\hat{\tilde{b}}} &= iG_0\hat{\tilde{a}} + iG_1\hat{\tilde{a}}^\dagger + i\tilde{G}_0\hat{\tilde{b}} + i\tilde{G}_1\hat{\tilde{b}}^\dagger - \frac{\gamma_m}{2}\hat{\tilde{b}} + \sqrt{\gamma_m}\hat{\tilde{b}}_{in}\end{aligned} \tag{4.4}$$

Where,

$$\begin{aligned}G_0 &= 2g_0[(b_{-1}+b_1)(a_{-1}+a_1) + 2b_0a_0] \\ G_1 &= 2g_0[(b_{-1}+b_1)a_0 + 2b_0a_1] \\ \tilde{G}_0 &= 2g_0(a_{-1}^2 + a_0^2 + a_1^2) \\ \tilde{G}_1 &= 2g_0(a_0a_1 + a_0a_{-1})\end{aligned} \tag{4.5}$$

Next, defining the quadrature fluctuation operators as $\delta\hat{\tilde{Q}}_{\mathcal{O}=\hat{\tilde{a}},\hat{\tilde{b}}} = \frac{\hat{\tilde{\mathcal{O}}}\pm\hat{\tilde{\mathcal{O}}}^\dagger}{\sqrt{2}}$. Similarly, quadrature noise operators are written as $\delta\hat{\tilde{Q}}^{in}_{\mathcal{O}=\hat{\tilde{a}},\hat{\tilde{b}}} = \frac{\hat{\tilde{\mathcal{O}}}_{in}\pm\hat{\tilde{\mathcal{O}}}^\dagger_{in}}{\sqrt{2}}$. Here, $\hat{\tilde{Q}}$ and $\hat{\tilde{Q}}_{in}$ are respectively the position or momentum quadrature and the corresponding noise associated with it. Thus, the quadrature fluctuations evolve in time as,

$$\begin{aligned}\delta\dot{\hat{\tilde{X}}}_a &= -G_-\delta\hat{\tilde{Y}}_b - \frac{\kappa}{2}\delta\hat{\tilde{X}}_a + \sqrt{\kappa}\delta\hat{\tilde{X}}_a^{in} \\ \delta\dot{\hat{\tilde{Y}}}_a &= G_+\delta\hat{\tilde{X}}_b - \frac{\kappa}{2}\delta\hat{\tilde{Y}}_a + \sqrt{\kappa}\delta\hat{\tilde{Y}}_a^{in} \\ \delta\dot{\hat{\tilde{X}}}_b &= -G_-\delta\hat{\tilde{Y}}_a - \frac{\gamma_m}{2}\delta\hat{\tilde{X}}_b - \tilde{G}_-\delta\hat{\tilde{Y}}_b + \sqrt{\gamma_m}\delta\hat{\tilde{X}}_b^{in} \\ \delta\dot{\hat{\tilde{Y}}}_b &= G_+\delta\hat{\tilde{X}}_a + \tilde{G}_+\delta\hat{\tilde{X}}_b - \frac{\gamma_m}{2}\delta\hat{\tilde{Y}}_b + \sqrt{\kappa}\delta\hat{\tilde{Y}}_b^{in}\end{aligned} \tag{4.6}$$

More concisely,

$$\begin{pmatrix}\delta\dot{\hat{\tilde{X}}}_a \\ \delta\dot{\hat{\tilde{Y}}}_a \\ \delta\dot{\hat{\tilde{X}}}_b \\ \delta\dot{\hat{\tilde{Y}}}_b\end{pmatrix} = \begin{pmatrix}-\frac{\kappa}{2} & 0 & 0 & -G_- \\ 0 & -\frac{\kappa}{2} & G_+ & 0 \\ 0 & -G_- & -\frac{\gamma_m}{2} & -\tilde{G}_- \\ G_+ & 0 & \tilde{G}_+ & -\frac{\gamma_m}{2}\end{pmatrix}\begin{pmatrix}\delta\hat{\tilde{X}}_a \\ \delta\hat{\tilde{Y}}_a \\ \delta\hat{\tilde{X}}_b \\ \delta\hat{\tilde{Y}}_b\end{pmatrix} + \begin{pmatrix}\sqrt{\kappa}\delta\hat{\tilde{X}}_a^{in} \\ \sqrt{\kappa}\delta\hat{\tilde{Y}}_a^{in} \\ \sqrt{\gamma_m}\delta\hat{\tilde{X}}_b^{in} \\ \sqrt{\gamma_m}\delta\hat{\tilde{Y}}_b^{in}\end{pmatrix}, \tag{4.7}$$

with $G_\pm = G_0 \pm G_1$ and $\tilde{G}_\pm = \tilde{G}_0 \pm \tilde{G}_1$. Here, drift matrix $\tilde{M} = \begin{pmatrix}-\frac{\kappa}{2} & 0 & 0 & -G_- \\ 0 & -\frac{\kappa}{2} & G_+ & 0 \\ 0 & -G_- & -\frac{\gamma_m}{2} & -\tilde{G}_- \\ G_+ & 0 & \tilde{G}_+ & -\frac{\gamma_m}{2}\end{pmatrix}$ and $\tilde{N}(t) = \begin{pmatrix}\sqrt{\kappa}\delta\hat{\tilde{X}}_a^{in} & \sqrt{\kappa}\delta\hat{\tilde{Y}}_a^{in} & \sqrt{\gamma_m}\delta\hat{\tilde{X}}_b^{in} & \sqrt{\gamma_m}\delta\hat{\tilde{Y}}_b^{in}\end{pmatrix}^T$.

4.2 Without Rotating Wave Approximation

Without ignoring the non-stationary terms, the time evolution of quadrature fluctuation can be written as,

$$\begin{aligned}\delta\dot{\hat{X}}_a &= -\frac{\kappa}{2}\delta\hat{X}_a + \Delta_a\delta\hat{Y}_a - 8g_o\,\mathrm{Re}[\beta]\,\mathrm{Im}[\alpha]\delta\hat{X}_b + \sqrt{\kappa}\delta\hat{X}_a^{in} \\ \delta\dot{\hat{Y}}_a &= -\Delta_a\delta\hat{X}_a - \frac{\kappa}{2}\delta\hat{Y}_a + 8g_o\,\mathrm{Re}[\beta]\,\mathrm{Re}[\alpha]\delta\hat{X}_b + \sqrt{\kappa}\delta\hat{Y}_a^{in}\end{aligned} \tag{4.8}$$

$$\begin{aligned}\delta\dot{\hat{X}}_b &= \omega_m\delta\hat{Y}_b - \frac{\gamma_m}{2}\delta\hat{X}_b + \sqrt{\gamma_m}\delta\hat{X}_b^{in} \\ \delta\dot{\hat{Y}}_b &= (-\omega_m + 4g_o|\alpha|^2)\delta\hat{X}_b + 8g_o\,\mathrm{Re}[\beta]\,\mathrm{Re}[\alpha]\delta\hat{X}_a + 8g_o\,\mathrm{Re}[\beta]\,\mathrm{Im}[\alpha]\delta\hat{Y}_a - \frac{\gamma_m}{2}\delta\hat{Y}_b + \sqrt{\kappa}\delta\hat{Y}_b^{in}\end{aligned} \tag{4.9}$$

Drift matrix for the system takes a form,

$$M = \begin{pmatrix} -\frac{\kappa}{2} & \Delta_a & -8g_o\,\mathrm{Re}[\beta]\,\mathrm{Im}[\alpha] & 0 \\ -\Delta_a & -\frac{\kappa}{2} & 8g_o\,\mathrm{Re}[\beta]\,\mathrm{Re}[\alpha] & 0 \\ 0 & 0 & -\frac{\gamma_m}{2} & \omega_m \\ 8g_o\,\mathrm{Re}[\beta]\,\mathrm{Re}[\alpha] & 8g_o\,\mathrm{Re}[\beta]\,\mathrm{Im}[\alpha] & -\omega_m + 4g_o|\alpha|^2 & -\frac{\gamma_m}{2} \end{pmatrix} \tag{4.10}$$

4.3 Covariance Matrix

The correlations between the position and momentum quadrature fluctuations can be written in terms of the covariance matrix V, whose elements are $V_{kk'} = \langle u_k u_{k'} + u_k u_{k'}\rangle/2$, where $u = (\delta\hat{X}_a, \delta\hat{Y}_a, \delta\hat{X}_b, \delta\hat{Y}_b)^T$. These correlations obey the equation of motion $\dot{V} = M.V + V.M^T + D$, where M is the Drift matrix we already derived and D is the noise matrix consisting of input noise quadratures $D = Diag[\kappa(n_a + 1/2), \kappa(n_a + 1/2), \gamma_m(n_m + 1/2), \gamma_m(n_m + 1/2)]$.

4.4 Routh-Hurwitz Criterion

Stability refers to a time-independent state of motion while dynamic stability refers to a time dependent state of motion. This dynamic stability is quantified by the Routh-Hurwitz criterion [8]. This criterion provides a way to determine the dynamical stability of the solutions to the equations of motion of a system. We apply R-H criterion to the polynomial of the eigenvalues of the drift matrix M.

$$Det(M - \lambda I) = \lambda^4 + a\lambda^3 + b\lambda^2 + c\lambda + d \tag{4.11}$$

The necessary and sufficient condition of stability requires that each eigenvalue of matrix M has only negative real part. This is possible if,

1. All the coefficients of the characteristic equation are positive.

2. Determinant of the Hurwitz matrices $|H_i|$ are positive, where the Hurwitz matrices are defined as,

$$H_1 = |a|, H_2 = \begin{pmatrix} a & 1 \\ c & b \end{pmatrix} \quad \text{and so on.} \tag{4.12}$$

In order for our quadratically coupled optomechanical system to be dynamically stable, the Routh-Hurwitz criterion implies the following inequalities:

$$\begin{aligned} \gamma + \kappa &> 0, \\ \frac{1}{4}\left(\gamma^2 + 4\gamma\kappa + \kappa^2\right) + 2G_-G_+ + \tilde{G}_-\tilde{G}_+ &> 0, \\ \tilde{G}_-\tilde{G}_+\kappa + \left(\frac{1}{4}\gamma\kappa + G_-G_+\right)(\gamma + \kappa) &> 0, \\ \frac{\kappa^2}{16}\left(4\tilde{G}_-\tilde{G}_+ + \gamma^2\right) + G_-^2G_+^2 + \frac{\gamma\kappa}{2}G_-G_+ &> 0. \end{aligned} \tag{4.13}$$

Now that the covariance matrix has been found and the Routh-Hurwitz criteria have been formulated, the variance in the position and momentum quadrature can be quantified from the covariance matrix for both the RWA (Sec. 4.1) and without RWA (Sec. 4.2) cases.

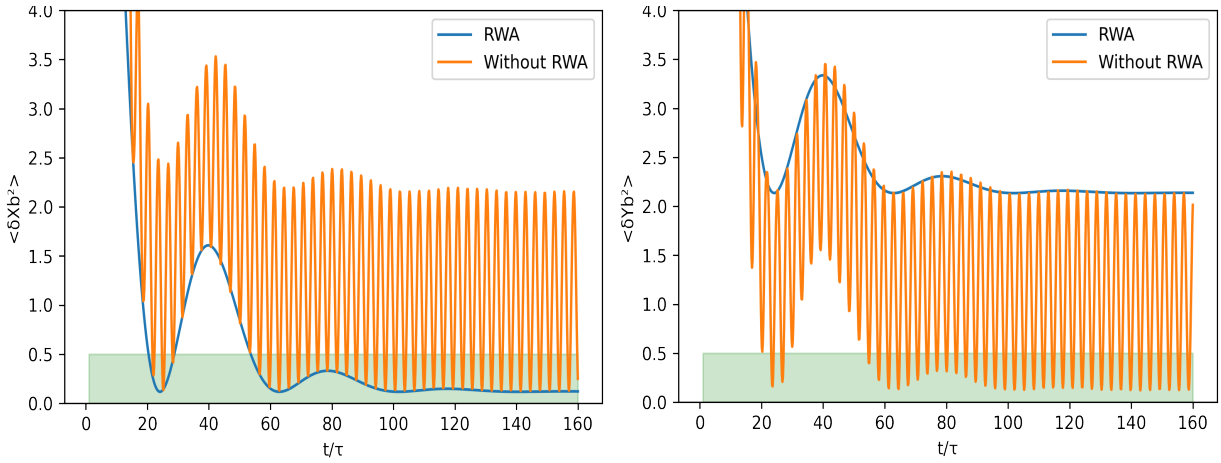

(a) (b)

Figure 4.1: The variance in fluctuations of position and momentum quadratures ($\delta\hat{X}_b$ and $\delta\hat{Y}_b$) with time. The parameters used are [2] $\Delta = \omega_m$, $g = 10^{-4}\omega_m$, $\Omega_a = \Omega_b = 2\omega_m$, $\kappa = 0.1\omega_m$, $\gamma = 10^{-6}\omega_m$, $a_0 = 2.0$, $a_{\pm 1} = 0.8$, $b_0 = 100$, $b_{-1} = 25$, $b_1 = 62.5$, $n_a = 0$ and $n_m = 10$. Here, the blue line is the behaviour calculated with the RWA and the orange line is that without the RWA. The green shaded region at the bottom corresponds to mechanical squeezing (below the standard quantum limit).

In the plots above, we check how the quadrature variances evolve with time by modulating the period of the driving amplitude in the range $[0, 100\tau]$. Clearly, without using RWA, the position and momentum quadratures get squeezed at regular intervals and at a long time limit this process occurs at a frequency determined by the modulation frequency of the external driving amplitude. This is in agreement with the Floquet theorem we discussed before, which states that in the long time limit the amplitude of the cavity and the mechanical mode achieve the same oscillation frequency as one for the external periodic driving $\epsilon_L(t)$. If we consider the RWA, we can safely get rid of the non-stationary terms in the evolution dynamics, then the frequency of squeezing is no longer the same as the frequency of $\epsilon_L(t)$, rather the former's magnitude falls abruptly below the standard quantum limit. However, in both these cases the magnitude of squeezing obtained stays almost the same.

4.5 Squeezing as a result of competing effect of two parameters

Now, we introduce an intuitive way of understanding the steady-state squeezing generated in our system. For equal sideband amplitudes ($G_0 = G_1$), the cavity is coupled to the mechanical quadrature $\hat{X}_b$. If $G_0 \neq G_1$, the cavity now couples to a new mechanical operator,

the Bogoliubov mode operator β. For that Bogoliubov mode $\hat{\beta} = \cosh r\hat{\tilde{b}} + \sinh r\hat{\tilde{b}}^\dagger$ where $\tanh r = \frac{G_1}{G_0}$.
The QLEs in Eq. (4.4) become,

$$\dot{\hat{\tilde{a}}} = i\cosh r(\hat{\beta}G_0 + \hat{\beta}^\dagger G_1) - i\sinh r(\hat{\beta}^\dagger G_0 + \hat{\beta}G_1) - \frac{\kappa}{2}\hat{\tilde{a}} + \sqrt{\kappa}\hat{\tilde{a}}_{in}(t) \tag{4.14}$$

Now, we take $\mathcal{G} = \sqrt{G_0^2 - G_1^2}$. Hence, $\cosh r = \frac{G_0}{\mathcal{G}}$ and $\sinh r = \frac{G_1}{\mathcal{G}}$. Thus,

$$\dot{\hat{\tilde{a}}} = i\hat{\beta}\mathcal{G} - \frac{\kappa}{2}\hat{\tilde{a}} + \sqrt{\kappa}\hat{\tilde{a}}_{in}(t) \tag{4.15}$$

Next, $\dot{\hat{\tilde{b}}} = iG_0\hat{\tilde{a}} + iG_1\hat{\tilde{a}}^\dagger + i\tilde{G_0}\hat{\tilde{b}} + i\tilde{G_1}\hat{\tilde{b}}^\dagger - \frac{\gamma_m}{2}\hat{\tilde{b}} + \sqrt{\gamma_m}\hat{\tilde{b}}_{in}$.
Substitute $\hat{\beta}$ and proceeding as before, we can find

$$\begin{aligned}\dot{\hat{\tilde{\beta}}} = i\mathcal{G}\hat{\tilde{a}} - \frac{\gamma_m}{2}\hat{\beta} + \sqrt{\gamma_m}\hat{\beta}_{in}(t) + i\Big[\Big(\frac{G_0^2+G_1^2}{\mathcal{G}^2}\Big)\tilde{G}_0 - \frac{2G_1G_0}{\mathcal{G}^2}\tilde{G}_1\Big]\hat{\beta} \\ + i\Big[\Big(\frac{G_0^2+G_1^2}{\mathcal{G}^2}\Big)\tilde{G}_1 - \frac{2G_1G_0}{\mathcal{G}^2}\tilde{G}_0\Big]\hat{\beta}^\dagger\end{aligned} \tag{4.16}$$

Here, $\hat{\beta}_{in} = \cosh r\hat{\tilde{b}}_{in} + \sinh r\hat{\tilde{b}}_{in}^\dagger$ is the noise operator in the bogoliubov mode. Now, qudrature fluctuations $\delta\hat{\tilde{X}}$ and $\delta\hat{\tilde{Y}}$ evolve as:

$$\begin{pmatrix} \delta\dot{\hat{\tilde{X}}}_a \\ \delta\dot{\hat{\tilde{Y}}}_a \\ \delta\dot{\hat{\tilde{X}}}_\beta \\ \delta\dot{\hat{\tilde{Y}}}_\beta \end{pmatrix} = \begin{pmatrix} -\frac{\kappa}{2} & 0 & 0 & -\mathcal{G} \\ 0 & -\frac{\kappa}{2} & \mathcal{G} & 0 \\ 0 & -\mathcal{G} & -\frac{\gamma_m}{2} & \Big(\frac{G_+}{G_-}\Big)\tilde{G}_- \\ \mathcal{G} & 0 & \Big(\frac{G_-}{G_+}\Big)\tilde{G}_- & -\frac{\gamma_m}{2} \end{pmatrix} \begin{pmatrix} \delta\hat{\tilde{X}}_a \\ \delta\hat{\tilde{Y}}_a \\ \delta\hat{\tilde{X}}_\beta \\ \delta\hat{\tilde{Y}}_\beta \end{pmatrix} + \begin{pmatrix} \sqrt{\kappa}\delta\hat{\tilde{X}}_a^{in} \\ \sqrt{\kappa}\delta\hat{\tilde{Y}}_a^{in} \\ \sqrt{\gamma_m}\delta\hat{\tilde{X}}_\beta^{in} \\ \sqrt{\gamma_m}\delta\hat{\tilde{Y}}_\beta^{in} \end{pmatrix} \tag{4.17}$$

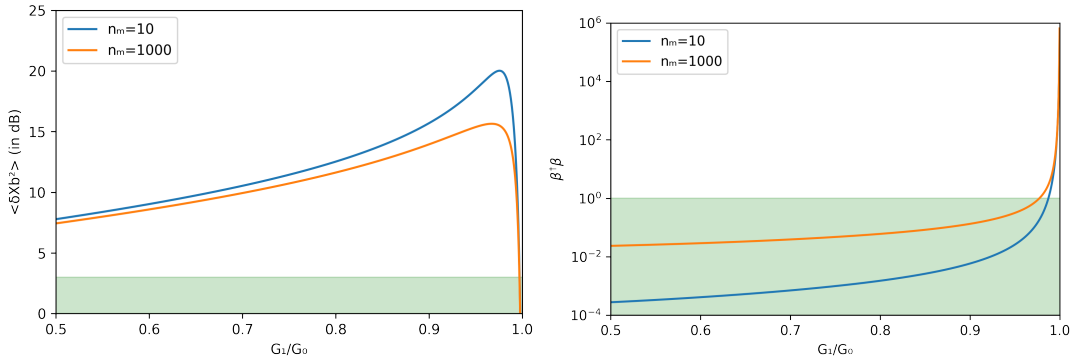

(a) (b)

Figure 4.2: (a) Variance in Position Quadrature $\langle \delta \hat{\hat{X}}_b^2 \rangle$ and (b) the number of atoms in the Bogoliubov Modes $\hat{\beta}$ plotted with respect to the ratio of the coupling strengths of the side-bands $\frac{G_1}{G_0}$ for different occupancy of the mechanical mode ($n_m = 10$ and $n_m = 1000$). Other parameters are same as in Figure 4.1. Here, the blue line is the behaviour calculated with the RWA and the orange line is that without the RWA. The green shaded region at the bottom in (a) corresponds to mechanical squeezing and red shaded region at the bottom in (b) corresponds to cooling of the bogoliubov mode for $\langle \beta^\dagger \beta \rangle < 1$

To ensure stability, from Sec. 4.4 we can reduce the constraint to $G_1 < G_0$. After transformaing the system Hamiltonian Eq. (3.5) to the rotated frame and then linearizing it Eq. (3.6), we substitute the bogoliubov operator. This leads to the Hamiltonian of the following form

$$\mathcal{H} = -\mathcal{G}(\hat{\tilde{a}}^\dagger \hat{\beta} + \text{h.c.}) \tag{4.18}$$

This is the well known beam-splitter Hamiltonian which describes energy exchange between the mechanical and the cavity mode. It is widely applied to implement optomechanical sideband cooling of the mechanical mode [9, 10]. Thus, the bogoliubov mode $\hat{\beta}$ undergoes ground-state cooling by interacting with the cavity mode $\hat{\tilde{a}}$. The squeezing parameter $r = \tanh^{-1}[\frac{G_1}{G_0}]$ increases with an increase in G_1 for a given G_0. This causes the squeezing of the mechanical mode to be enhanced, which is clear from Figure 4.2. Now, the enhanced coupling rate between the optical field and the mechanical oscillator is now given by $\mathcal{G} = \sqrt{G_0^2 - G_1^2}$. With an increase in G_1 this value steadily decreases and finally becomes zero. At this point the Bogoliubov cooling can no longer happen, which is shown by the sharp increase in its occupancy $\hat{\beta}^\dagger \hat{\beta}$ for $\frac{G_1}{G_0} \to 1$. After this stage, the effects of thermal noise kick in making it impossible to achieve high degree of squeezing. This is shown by the abrupt fall in the value of $\langle \delta \hat{\hat{X}}_b^2 \rangle$ almost competing with the rise in occupancy of the bogoliubov mode. Thus, there is an optimum value of the sideband ratio $\frac{G_1}{G_0}$ for which the squeezing achieved in maximum.

4.6 Optimal side-band ratio

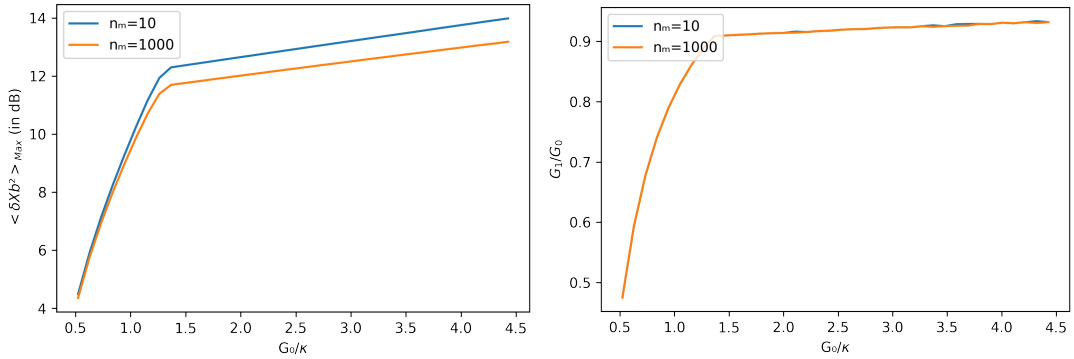

(a) (b)

Figure 4.3: (a) Maximized Variance in Position Quadrature $\langle \delta \hat{\tilde{X}}_b^2 \rangle$ and (b) Optimal side-band ratio $\frac{G_1}{G_0}$ plotted with respect to the coupling strength of the side-band G_0 for different occupancy of the mechanical mode ($n_m = 10$ and $n_m = 1000$). Other parameters are same as in Figure 4.1.

In Figure 4.2, we have seen, for a certain critical value of the side-band ratio, the mechanical squeezing in the quadrature obtained is maximum. Now, in Figure 4.3 (a), we vary the values of the G_0 and look at the variation of the maximum value of quadrature variance $\langle \delta \hat{\tilde{X}}_b^2 \rangle$. Another noteworthy observation is that, with an increase in the average number of atoms in the mechanical mode, the maximized $\langle \delta \hat{\tilde{X}}_b^2 \rangle$ decreases. This can be explained from the effect of thermal noise in the mechanical bath as stated previously.
To achieve mechanical squeezing of high magnitude, optimizing the side-band ratio is necessary. Thus, in Figure 4.3(b), we numerically optimize the side-band ratio $\frac{G_1}{G_0}$ by plotting its value corresponding to the highest degree of squeezing obtained in Figure 4.2(a) with respect to G_0. The coupling given by $\mathcal{G} = \sqrt{G_0^2 - G_1^2}$ increases with an increase in G_0, for a specific side-band ratio. As a result, the bogoliubov cooling is much more enhanced. This behaviour is demonstrated by the tendency of G_1/G_0 to attain a value very close to 1 but not exactly 1.

Chapter 5

Analytical and Numerical Solutions

5.1 Analytical Solution (under Adiabatic Approximation)

The system dynamics under the rotating-wave approximation as we derived in Sec. 4.5 is time-independent. In the limit of weak optomechanical coupling (i.e. the rate of decay of the optical mode κ is much higher than the coupling strength $\mathcal{G}$), the cavity photons fizzle out faster than the optomechanical interaction. So, the cavity field follows mechanical motion adiabatically. We can eliminate the cavity mode $\hat{\tilde{a}}$ under the adiabatic approximation (i.e. $\dot{\hat{\tilde{a}}} = 0$)[11].
Let us now analytically solve for the position quadrature variance of the mechanical mode. Using Adiabatic Approximation we can write Eq. (4.15) as

$$\begin{aligned} 0 &= i\hat{\beta}\mathcal{G} - \frac{\kappa}{2}\hat{\tilde{a}} + \sqrt{\kappa}\hat{\tilde{a}}_{in}(t) \\ \Rightarrow \hat{\tilde{a}} &= \frac{2i\mathcal{G}}{\kappa}\hat{\beta} + \frac{2}{\sqrt{\kappa}}\hat{\tilde{a}}_{in}(t) \end{aligned} \tag{5.1}$$

Now, substituting Eq. (5.1) in Eq. (4.16),

$$\begin{aligned} \dot{\hat{\beta}} \simeq -h\hat{\beta} + \frac{2i\mathcal{G}}{\sqrt{\kappa}}\hat{\tilde{a}}_{in}(t) + \sqrt{\gamma_m}\hat{\beta}_{in}(t) + i\Big[\Big(\frac{G_0^2+G_1^2}{\mathcal{G}^2}\Big)\tilde{G}_0 - \frac{2G_1G_0}{\mathcal{G}^2}\tilde{G}_1\Big]\hat{\beta} + \\ i\Big[\Big(\frac{G_0^2+G_1^2}{\mathcal{G}^2}\Big)\tilde{G}_1 - \frac{2G_1G_0}{\mathcal{G}^2}\tilde{G}_0\Big]\hat{\beta}^\dagger \end{aligned} \tag{5.2}$$

Where, $h = \frac{2\mathcal{G}^2}{\kappa} + \frac{\gamma_m}{2}$
As shown is Appendix - B, we show that the position variance in the bogoliubov mode can be written as,

$$\begin{aligned} \langle \delta\hat{X}_\beta^2 \rangle = \frac{h}{2\left(\tilde{G}_-^2 - h^2\right)}\Bigg\{ \gamma\left(n_b + \frac{1}{2}\right)\left(\frac{\tilde{G}_- G_+}{G_- h}e^{-2r} - e^{2r}\right) \\ - \frac{4\mathcal{G}^2}{\kappa}\left(n_a + \frac{1}{2}\right)\left(1 + \frac{\tilde{G}_- G_+}{G_- h}\right)\Bigg\} \end{aligned} \tag{5.3}$$

Hence, the steady-state solution for the variance of position quadrature,

$$\begin{aligned} \hat{X}_\beta^2 &= \frac{1}{2}(\cosh r + \sinh r)^2(\hat{\tilde{b}}^\dagger + \hat{\tilde{b}}) = e^{2r}\hat{\tilde{X}}_b^2 \\ \Rightarrow \langle \hat{\tilde{X}}_b^2 \rangle_s &= e^{-2r}\langle \delta\hat{X}_\beta^2 \rangle \end{aligned} \tag{5.4}$$

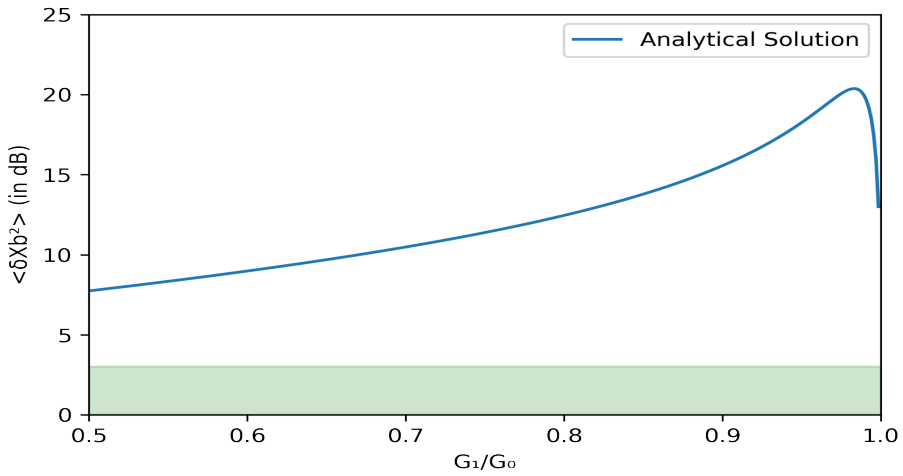

Figure 5.1: Variance in Position Quadrature $\langle \delta\hat{\tilde{X}}_b^2 \rangle$ obtained from the approximate solution Eq. (5.4), plotted with respect to the ratio of the coupling strengths of the side-bands $\frac{G_1}{G_0}$ for $n_m = 10$. Here, the parameters are same as in Figure 4.1.

To check for the consistency of our previous results obtained in Sec. 4.5, we plot the analytically obtained steady state position variance with respect to the side-band ratio. Clearly, the nature of the plot for $\langle \hat{\tilde{X}}_b^2 \rangle$ obtained in Figure 4.2 matches with that in Figure 5.1.

5.2 Numerical Solution

Next, we check for the accuracy of the analytical result we derived under adiabatic approximation, we now find the exact numerical solution for the steady-state position variance $\langle \delta\hat{\tilde{X}}_b^2 \rangle$. From Eq. (4.7), $\dot{\tilde{R}}(t) = \tilde{M}\tilde{R}(t) + \tilde{N}(t)$. We know that, in the Fourier domain, $\frac{d}{dt}\tilde{R}(t) = -i\omega\tilde{R}(t)$. Hence,

$$\begin{aligned} -i\omega\tilde{R}(t) &= \tilde{M}\tilde{R}(\omega) + \tilde{N}(\omega) \\ \Rightarrow(-i\omega\mathbb{I} - M)\tilde{R}(\omega) &= \tilde{N}(\omega) \\ \Rightarrow\tilde{R}(\omega) &= (i\omega\mathbb{I} + M)^{-1}\tilde{N}(\omega) \end{aligned} \tag{5.5}$$

Now, the equation above is a system of 4 linear equations. However, we only need expression for $\delta\tilde{X}_b$,

$$\delta\tilde{X}_b = A(\omega)\delta\tilde{X}_a^{in} + B(\omega)\delta\tilde{Y}_a^{in} + E(\omega)\delta\tilde{X}_b^{in} + F(\omega)\delta\tilde{Y}_b^{in} \tag{5.6}$$

The first two terms in the above expression arise from the vacuum noise in the cavity mode and the last two terms arise from the thermal noise in the mechanical mode. Now, we can solve Eq. (5.5) and obtain the fluctuation spectra of the position quadrature of the mechanical mode [See Appendix C],
Integrating $S_{\tilde{X}_b}(\omega)$ within the whole spectral regime ($\frac{1}{2\pi}\int_{-\infty}^{\infty} d\omega S_{\tilde{X}_b}(\omega)$), we can obtain the variance in position quadrature for the mechanical mode $\langle \hat{\tilde{X}}_b^2 \rangle_s$ in steady-state. Let us plot the numerically obtained steady-state position variance with respect to the side-band ratio,

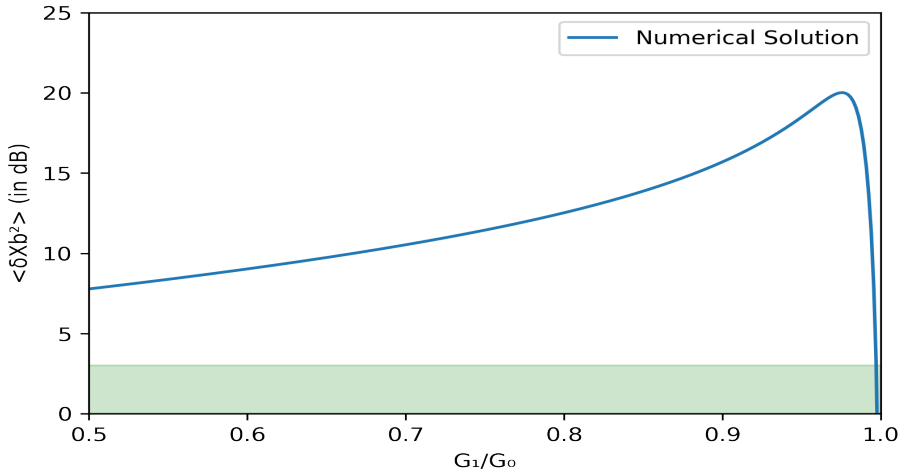

Figure 5.2: Variance in Position Quadrature $\langle \delta \hat{\tilde{X}}_b^2 \rangle$ obtained from numerical solution, plotted with respect to the ratio of the coupling strengths of the side-bands $\frac{G_1}{G_0}$ for $n_m = 10$. Here, the parameters are same as in Figure 4.1.

Clearly, this result exactly matches the nature of $\langle \hat{\tilde{X}}_b^2 \rangle$ we had previously obtained in Section 4.5.
Now, again we try to find the optimal value of the side-band ratio $\frac{G_1}{G_0}|_{opt}$ by calculating $\frac{d\langle \hat{\tilde{X}}_b^2 \rangle_s}{d(\frac{G_1}{G_0})} = 0$. I have used the analytically calculated value of position quadrature variance from Eq. (5.4). This gives us a transcendental equation which is quite difficult to solve.
To simplify things, we define a parameter called Cooperativity. It quantifies how efficient a system is in exchanging photons and phonons. Assuming that the Cooperativity $\mathcal{C} = \frac{4G_0^2}{\kappa\gamma}$ is very large ($\mathcal{C} \gg 1$), we can approximate $e^{-2r} \simeq \sqrt{\frac{n_m+\frac{1}{2}}{2\mathcal{C}}}$ [1]. Now, substituting in the transcendental equation, we get an expression for $\frac{G_1}{G_0}|_{opt}$ which can be plotted with respect to the side-band G_0.

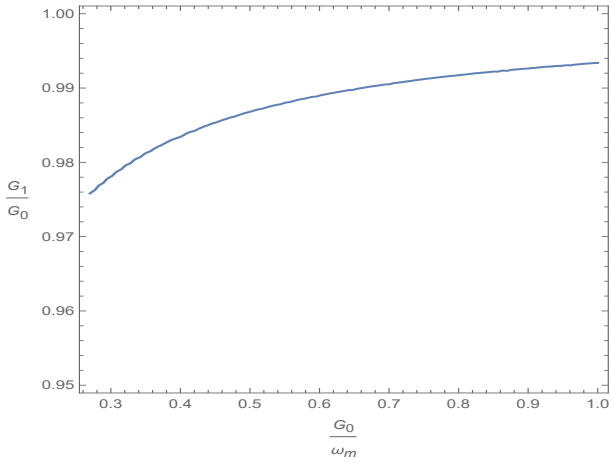

Figure 5.3: Optimal ratio of the side-band strength plotted with respect to the side-band G_0 as obtained from the analytical solution in Eq. (5.4). The parameters are same as in Figure 4.1.

In Figure 5.3, we find that the optimal $\frac{G_1}{G_0}$ slowly approaches unity as the side-band strength G_0 increases but never actually reaches unity because of the effects of thermal noise as explained in Section 4.6.

Now, let's see how robust the mechanical squeezing obtained using this scheme is. For that, we plot the numerical solution for $\langle \hat{\tilde{X}}_b^2 \rangle_s$ obtained by integrating Eq. (C.5), as a function of the thermal phonon occupation number n_m.

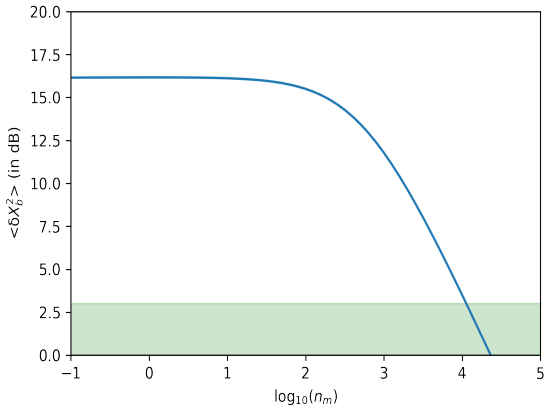

Figure 5.4: Steady state variance in position quadrature $\langle \hat{\tilde{X}}_b^2 \rangle_s$ is plotted with varying occupancy of the mechanical mode n_m for an optimised side-band ratio. Here, The green shaded region at the bottom in corresponds to mechanical squeezing. Other parameters are same as in Figure 4.1

In Figure 5.4, a strong mechanical squeezing ($\sim$ 16 dB) is achieved for a low occupancy of the thermal bath. At higher bath temperature (corresponding phonon number $\sim 10^4$),

the steady-state mechanical squeezing is still beyond the 3 dB limit. This demonstrates the robustness of our scheme.

Chapter 6

Discussion

In this dissertation, we have investigated an efficient way of generating a high degree of quadrature squeezing in a cavity optomechanical system by modulating the laser field amplitude periodically. We see that the dissipative dynamics causes the Bogoliubov mode to cool down to its ground state. As this ground state corresponds to a squeezed state, squeezing is generated via dissipation. Squeezing obtained is maximum when conflicting effect of two parameters ($\langle \delta \hat{X}_b^2 \rangle$ and $\langle \hat{\beta}^\dagger \hat{\beta} \rangle$) gets optimized by changing the ratio of the side-band strengths of the coupling parameter.

To better understand how the system evolves with time, we start by solving the system dynamics both in under the rotating wave approximation as well as without it. We see that, in the long time limit, the variance in the position and momentum quadratures follow the modulating frequency of the optical field amplitude. However, under the rotating approximation, the variance goes well below the standard 3-dB quantum limit.

Next, we have analyzed the quadrature squeezing analytically (under adiabatic approximation) as well as numerically by integrating the fluctuation spectra in the whole frequency domain. With that, we showed that the squeezed quadrature fluctuations of the mechanical mode grows monotonically with the increase in $\frac{G_1}{G_0}$ and then falls abruptly over a certain critical value.

Lastly, we concluded that this present scheme is extremely robust and for an optimized value of the ratio of the side-bands of the optomechanical coupling parameter G, squeezing is achievable which is even for a high occupation factor of the mechanical mode.

Appendices

Appendix A

Table of variable definitions

$\hat{a}$		optical mode annihilation operator
l		optical cavity length (base)
ω_a		optical mode frequency (base)
κ		optical mode decay rate
$\hat{b}$		mechanical mode annihilation operator
x_{zpf}	$\sqrt{\frac{\hbar}{2m\omega_m}}$	mechanical zero-point position
p_{zpf}	$\sqrt{\frac{\hbar m\omega_m}{2}}$	mechanical zero-point momentum
m		mechanical mode mass
ω_m		mechanical mode frequency
γ_m		mechanical mode decay rate
g_0	$\frac{\omega_a x_{zpf}}{\sqrt{2}l}$	optomechanical coupling rate
ϵ_L	$\sqrt{\frac{\kappa P_L}{\hbar\omega_L}}$	laser amplitude
P_L		laser input power
ω_L	$\frac{2\pi c}{\lambda_L}$	laser frequency
λ_L		laser wavelength
δ_a	$\omega_a - \omega_L$	optical detuning from the laser frequency

Appendix B

Steady state fluctuation of the mechanical mode

The fluctuation in postion in Bogoliubov Mode is given by the operator $\delta\hat{X}_\beta = \frac{\hat{\beta}+\hat{\beta}^\dagger}{\sqrt{2}}$ and $\delta\hat{Y}_\beta = \frac{\hat{\beta}-\hat{\beta}^\dagger}{\sqrt{2}i}$. From Eq. (5.2),

$$\begin{aligned}\delta\dot{\hat{X}}_\beta &= -h\delta\hat{X}_\beta - \frac{2}{\sqrt{\kappa}}\mathcal{G}\hat{\tilde{Y}}_a^{in}(t) + \sqrt{\frac{\gamma_m}{2}}[\hat{\beta}_{in}^\dagger(t) + \hat{\beta}_{in}(t)] + \Big(\frac{G_0+G_1}{G_0-G_1}\Big)(\tilde{G}_1-\tilde{G}_0)\delta\hat{Y}_\beta \\ \delta\dot{\hat{Y}}_\beta &= -h\delta\hat{Y}_\beta + \frac{2}{\sqrt{\kappa}}\mathcal{G}\hat{\tilde{X}}_a^{in}(t) + \sqrt{\frac{\gamma_m}{2}}\Big[\frac{\hat{\beta}_{in}(t)-\hat{\beta}_{in}^\dagger(t)}{i}\Big] + \Big(\frac{G_0-G_1}{G_0+G_1}\Big)(\tilde{G}_1+\tilde{G}_0)\delta\hat{X}_\beta\end{aligned} \tag{B.1}$$

Here, we can assign the terms $-\frac{2}{\sqrt{\kappa}}\mathcal{G}\hat{\tilde{Y}}_a^{in}(t)$, $\sqrt{\frac{\gamma_m}{2}}[\hat{\beta}_{in}^\dagger(t)+\hat{\beta}_{in}(t)]$ and $\sqrt{\frac{\gamma_m}{2}}\Big[\frac{\hat{\beta}_{in}(t)-\hat{\beta}_{in}^\dagger(t)}{i}\Big]$ are assigned to $\mathcal{F}_1(t)$, $\mathcal{F}_2(t)$ and $\mathcal{F}_3(t)$ respectively, where $\mathcal{F}_i$ are the effective quantum langevin forces. The correlation functions of these forces can be calculated as

$$\langle\mathcal{F}_1(t)\mathcal{F}_1(t')\rangle = (-\frac{2}{\sqrt{\kappa}}\mathcal{G})^2\int d\omega\langle\hat{\tilde{Y}}_a^{in}(t)\hat{\tilde{Y}}_a^{in}(t)\rangle e^{i\omega(t-t')} \tag{B.2}$$

First, let's calculate $\langle\hat{\tilde{Y}}_a^{in}(t)\hat{\tilde{Y}}_a^{in}(t)\rangle$,

$$\begin{aligned}\langle\hat{\tilde{Y}}_a^{in}(t)\hat{\tilde{Y}}_a^{in}(t)\rangle &= \frac{1}{2}(\hat{\tilde{a}}_{in}-\hat{\tilde{a}}_{in}^\dagger)(\hat{\tilde{a}}_{in}^\dagger-\hat{\tilde{a}}_{in}) \\ &= \frac{1}{2}[2(\hat{\tilde{a}}_{in}-\hat{\tilde{a}}_{in})+1] = (n_a+\frac{1}{2})\end{aligned} \tag{B.3}$$

Hence,

$$\langle\mathcal{F}_1(t)\mathcal{F}_1(t')\rangle = (-\frac{2\mathcal{G}}{\sqrt{\kappa}})^2(n_a+\frac{1}{2})\delta(t-t')$$

Again,

$$\langle\mathcal{F}_2(t)\mathcal{F}_2(t')\rangle = (\sqrt{\frac{\gamma_m}{2}})^2\int d\omega\langle(\hat{\beta}_{in}^\dagger(t)+\hat{\beta}_{in}(t))(\hat{\beta}_{in}(t)+\hat{\beta}_{in}^\dagger(t))\rangle e^{i\omega(t-t')} \tag{B.4}$$

Now, $\langle(\hat{\beta}_{in}^{\dagger}(t)+\hat{\beta}_{in}(t))(\hat{\beta}_{in}(t)+\hat{\beta}_{in}^{\dagger}(t))\rangle = 2e^{2r}(n_m+\frac{1}{2})$, Hence,

$$\langle \mathcal{F}_2(t)\mathcal{F}_2(t')\rangle = \gamma_m e^{2r}(n_m+\frac{1}{2})\delta(t-t')$$

Similarly,

$$\langle \mathcal{F}_3(t)\mathcal{F}_3(t')\rangle = -\gamma_m e^{-2r}(n_m+\frac{1}{2})\delta(t-t')$$

Now, we can write down the equations of the position and momentum quadrature fluctuations in the bogoliubov mode Eq. (B.1),

$$\frac{d}{dt}\langle\delta\hat{X}_\beta^2\rangle = -2h\langle\delta\hat{X}_\beta^2\rangle + \frac{4\mathcal{G}^2}{\kappa}(n_a+\frac{1}{2}) + \gamma_m e^{2r}(n_m+\frac{1}{2}) + 2\Big(\frac{G_0+G_1}{G_0-G_1}\Big)(\tilde{G}_1-\tilde{G}_0)\langle\delta\hat{Y}_\beta^2\rangle$$

and

$$\frac{d}{dt}\langle\delta\hat{Y}_\beta^2\rangle = -2h\langle\delta\hat{Y}_\beta^2\rangle + \frac{4\mathcal{G}^2}{\kappa}(n_a+\frac{1}{2}) - \gamma_m e^{2r}(n_m+\frac{1}{2}) + 2\Big(\frac{G_0-G_1}{G_0+G_1}\Big)(\tilde{G}_1+\tilde{G}_0)\langle\delta\hat{X}_\beta^2\rangle$$

Again, under adiabatic approximation, we take $\frac{d}{dt}\langle\delta\hat{X}_\beta^2\rangle = \frac{d}{dt}\langle\delta\hat{Y}_\beta^2\rangle = 0$. Hence,

$$\langle\delta\hat{X}_\beta^2\rangle = \frac{2\mathcal{G}^2}{\kappa h}(n_a+\frac{1}{2}) + \frac{\gamma_m}{2h}e^{2r}(n_m+\frac{1}{2}) + \Big(\frac{G_0+G_1}{G_0-G_1}\Big)\frac{(\tilde{G}_1-\tilde{G}_0)}{h}\langle\delta\hat{Y}_\beta^2\rangle \tag{B.5}$$

$$\langle\delta\hat{Y}_\beta^2\rangle = \frac{2\mathcal{G}^2}{\kappa h}(n_a+\frac{1}{2}) - \frac{\gamma_m}{2h}e^{2r}(n_m+\frac{1}{2}) + \Big(\frac{G_0-G_1}{G_0+G_1}\Big)\frac{(\tilde{G}_1+\tilde{G}_0)}{h}\langle\delta\hat{X}_\beta^2\rangle \tag{B.6}$$

Now solving these two coupled equations,

$$\begin{aligned}\langle\delta\hat{X}_\beta^2\rangle = \frac{h}{2\left(\tilde{G}_-^2-h^2\right)}\Bigg\{&\gamma\left(n_b+\frac{1}{2}\right)\left(\frac{\tilde{G}_-G_+}{G_-h}e^{-2r}-e^{2r}\right)\\ &-\frac{4\mathcal{G}^2}{\kappa}\left(n_a+\frac{1}{2}\right)\left(1+\frac{\tilde{G}_-G_+}{G_-h}\right)\Bigg\}\end{aligned} \tag{B.7}$$

Hence, the steady-state solution for the variance of position quadrature,

$$\begin{aligned}\hat{X}_\beta^2 &= \frac{1}{2}(\cosh r+\sinh r)^2(\hat{\tilde{b}}^\dagger+\hat{\tilde{b}}) = e^{2r}\hat{\tilde{X}}_b^2\\ &\Rightarrow \langle\hat{\tilde{X}}_b^2\rangle_s = e^{-2r}\langle\delta\hat{X}_\beta^2\rangle\end{aligned} \tag{B.8}$$

Appendix C

Position fluctuation spectra of the mechanical mode

The expression of quadrature fluctuation of the mechanical mode $\delta\tilde{X}_b$ we by solving Eq. (5.5) is of form,

$$\delta\tilde{X}_b = A(\omega)\delta\tilde{X}_a^{in} + B(\omega)\delta\tilde{Y}_a^{in} + E(\omega)\delta\tilde{X}_b^{in} + F(\omega)\delta\tilde{Y}_b^{in} \tag{C.1}$$

Here, the coefficients are as follows,

$$\begin{aligned}
A(\omega) &= -\frac{1}{\Lambda}8G_+\sqrt{\kappa}\tilde{G}_-(\kappa - 2i\omega), && \text{(C.2a)}\\
B(\omega) &= \frac{1}{\Lambda}4G_-\sqrt{\kappa}\left\{-4G_-G_+ + (2\omega + i\kappa)\,(2\omega + i\gamma_m)\right\}, && \text{(C.2b)}\\
C(\omega) &= \frac{1}{\Lambda}2(\kappa - 2i\omega)\sqrt{\gamma_m}\left\{4G_-G_+ + (\kappa - 2i\omega)\,(\gamma_m - 2i\omega)\right\}, && \text{(C.2c)}\\
D(\omega) &= -\frac{1}{\Lambda}4\tilde{G}_-(\kappa - 2i\omega)^2\sqrt{\gamma_m}, && \text{(C.2d)}
\end{aligned}$$

where $\Lambda = (\kappa - 2i\omega)^2\left\{-4\tilde{G}_-\tilde{G}_+ + (2\omega + i\gamma_m)^2\right\} + 8G_-G_+(2\omega + i\kappa)\,(2\omega + i\gamma_m) - 16G_-^2G_+^2$. In the fourier space, the correlation between the operators $\tilde{\mathcal{O}}_{a(b)}^{in}(\omega)$ can be given as:

$$\begin{aligned}
&\langle\hat{\tilde{X}}_a^{in}(\omega)\hat{\tilde{X}}_a^{in}(\Omega)\rangle = \langle\hat{\tilde{Y}}_a^{in}(\omega)\hat{\tilde{Y}}_a^{in}(\Omega)\rangle = \int dt\langle\hat{\tilde{Y}}_a^{in}(\omega)\hat{\tilde{Y}}_a^{in}(\Omega)\rangle e^{i\omega(\omega+\Omega)t} = (n_a + \frac{1}{2})2\pi\delta(\omega + \Omega)\\
&\langle\hat{\tilde{X}}_a^{in}(\omega)\hat{\tilde{Y}}_a^{in}(\Omega)\rangle = -\langle\hat{\tilde{Y}}_a^{in}(\omega)\hat{\tilde{X}}_a^{in}(\Omega)\rangle = i\pi\delta(\omega + \Omega)\\
&\langle\hat{\tilde{X}}_b^{in}(\omega)\hat{\tilde{X}}_b^{in}(\Omega)\rangle = \langle\hat{\tilde{Y}}_b^{in}(\omega)\hat{\tilde{Y}}_b^{in}(\Omega)\rangle = (n_m + \frac{1}{2})2\pi\delta(\omega + \Omega)\\
&\langle\hat{\tilde{X}}_b^{in}(\omega)\hat{\tilde{Y}}_b^{in}(\Omega)\rangle = -\langle\hat{\tilde{Y}}_b^{in}(\omega)\hat{\tilde{X}}_b^{in}(\Omega)\rangle = i\pi\delta(\omega + \Omega)
\end{aligned} \tag{C.3}$$

Fluctuation spectrum of the position quadrature in the mechanical mode $\delta\tilde{X}_b$ is given as,

$$S_{\tilde{X}_b}(\omega)\delta(\omega + \Omega) = \frac{1}{4\pi}(\langle\hat{\tilde{X}}_a(\omega)\hat{\tilde{X}}_a(\Omega)\rangle + \langle\hat{\tilde{X}}_b(\omega)\hat{\tilde{X}}_b(\Omega)\rangle) \tag{C.4}$$

Putting in the values of the correlations between the quadrature noise operators from Eq. (C.3),

$$\begin{aligned} S_{\tilde{X}_b}(\omega) = &\left[A\left(-\omega\right)A\left(\omega\right) + B\left(-\omega\right)B\left(\omega\right)\right]\left(n_a + \frac{1}{2}\right) \\ &+ \left[C\left(-\omega\right)C\left(\omega\right) + D\left(-\omega\right)D\left(\omega\right)\right]\left(n_m + \frac{1}{2}\right) \end{aligned} \tag{C.5}$$

Chapter 7

Bibliography

[1] A. Kronwald, F. Marquardt, and A. A. Clerk, "Arbitrarily large steady-state bosonic squeezing via dissipation," *Phys. Rev. A*, vol. 88, p. 063833, Dec 2013.

[2] C.-H. Bai, D.-Y. Wang, S. Zhang, S. Liu, and H.-F. Wang, "Strong mechanical squeezing in a standard optomechanical system by pump modulation," *Phys. Rev. A*, vol. 101, p. 053836, May 2020.

[3] B. P. Abbott, R. Abbott, R. Adhikari, and P. A. et. al., "LIGO: the laser interferometer gravitational-wave observatory," *Reports on Progress in Physics*, vol. 72, p. 076901, jun 2009.

[4] T. Accadia, F. Acernese, F. Antonucci, P. Astone, and G. B. et. al., "Calibration and sensitivity of the virgo detector during its second science run," *Classical and Quantum Gravity*, vol. 28, p. 025005, dec 2010.

[5] E. E. Wollman, C. U. Lei, A. J. Weinstein, J. Suh, A. Kronwald, F. Marquardt, A. A. Clerk, and K. C. Schwab, "Quantum squeezing of motion in a mechanical resonator," *Science*, vol. 349, no. 6251, pp. 952–955, 2015.

[6] C. Gardiner, P. Zoller, and P. Zoller, *Quantum noise: a handbook of Markovian and non-Markovian quantum stochastic methods with applications to quantum optics*. Springer Science & Business Media, 2004.

[7] G. Teschl, *Ordinary differential equations and dynamical systems*, vol. 140. American Mathematical Soc., 2012.

[8] A. Mari and J. Eisert, "Gently modulating optomechanical systems," *Phys. Rev. Lett.*, vol. 103, p. 213603, Nov 2009.

[9] I. Wilson-Rae, N. Nooshi, W. Zwerger, and T. J. Kippenberg, "Theory of ground state cooling of a mechanical oscillator using dynamical backaction," *Phys. Rev. Lett.*, vol. 99, p. 093901, Aug 2007.

[10] F. Marquardt, J. P. Chen, A. A. Clerk, and S. M. Girvin, "Quantum theory of cavity-assisted sideband cooling of mechanical motion," *Phys. Rev. Lett.*, vol. 99, p. 093902, Aug 2007.

[11] G. S. Agarwal and S. Huang, "Strong mechanical squeezing and its detection," *Phys. Rev. A*, vol. 93, p. 043844, Apr 2016.